Ultrasonics Sonochemistry 21 (2014) 401–408

Contents lists available at SciVerse ScienceDirect

Ultrasonics Sonochemistry

journal homepage: www.elsevier.com/locate/ultson

Ultrasound-induced emulsification of subcritical carbon dioxide/water with and without surfactant as a strategy for enhanced mass transport

Steven M. Cenci [a], Liam R. Cox [b], Gary A. Leeke [a,*]

[a] School of Chemical Engineering, University of Birmingham, Edgbaston, Birmingham B15 2TT, UK
[b] School of Chemistry, University of Birmingham, Edgbaston, Birmingham B15 2TT, UK

ARTICLE INFO

Article history:
Received 21 February 2013
Received in revised form 14 May 2013
Accepted 26 May 2013
Available online 3 June 2013

Keywords:
CO_2
Aqueous media
Subcritical
Emulsion
Mass transport
Hydrolysis

ABSTRACT

Pulsed ultrasound was used to disperse a biphasic mixture of CO_2/H_2O in a 1 dm^3 high-pressure reactor at 30 °C/80 bar. A view cell positioned in-line with the sonic vessel allowed observation of a turbid emulsion which lasted approximately 30 min after ceasing sonication. Within the ultrasound reactor, simultaneous CO_2-continuous and H_2O-continuous environments were identified. The hydrolysis of benzoyl chloride was employed to show that at similar power intensities, comparable initial rates ($1.6 \pm 0.3 \times 10^{-3}$ s^{-1} at 95 W cm^{-2}) were obtained with those reported for a 87 cm^3 reactor ($1.8 \pm 0.2 \times 10^{-3}$ s^{-1} at 105 W cm^{-2}), demonstrating the conservation of the physical effects of ultrasound in high-pressure systems (emulsification induced by the action of acoustic forces near an interface). A comparison of benzoyl chloride hydrolysis rates and benzaldehyde mass transport relative to the non-sonicated, 'silent' cases confirmed that the application of ultrasound achieved reaction rates which were over 200 times faster, by reducing the mass transport resistance between CO_2 and H_2O. The versatility of the system was further demonstrated by ultrasound-induced hydrolysis in the presence of the polysorbate surfactant, Tween, which formed a more uniform CO_2/H_2O emulsion that significantly increased benzoyl chloride hydrolysis rates. Finally, pulse rate was employed as a means of slowing down the rate of hydrolysis, further illustrating how ultrasound can be used as a valuable tool for controlling reactions in CO_2/H_2O solvent mixtures.

1. Introduction

One way of improving the separation between immiscible species following synthetic procedures, is to use a biphasic system involving an organic solvent and an aqueous phase [1,2]. Owing to its low critical point (31.1 °C/73.8 bar) and ease of separation upon depressurisation, subcritical or supercritical CO_2 may be employed usefully as a replacement for the organic phase [3,4]. Moreover, as the solvating power of CO_2 is confined to small, relatively non-polar compounds, the presence of a second aqueous phase can greatly increase the accessibility of hydrophilic species (e.g. salts), that are commonly employed in many organic chemistry reactions. Additionally, the reaction of CO_2 with water leads to the formation of carbonic acid, providing an intrinsic proton source (pH 3–4) [5,6], which may be advantageous for several processes [7].

Due to the presence of a liquid–liquid interfacial barrier, mass transfer rates in biphasic systems may be improved by increasing the interfacial area through the formation of an emulsion [8]. Emulsions of CO_2/H_2O (C/W) have the distinct advantage over conventional organic-phase emulsions of allowing the complete reversal to the biphase upon depressurisation of the system. Furthermore, the droplet size and stability of the emulsion may be controlled by specially-designed surfactant molecules allowing greater fine-tuning of the reaction system [9]. Dispersions of CO_2 and water, as emulsions or microemulsions [10], have been developed for a range of synthetic processes, including hydrogenations [11–14], hydroformylations [15], the synthesis of metal nanoparticles [16], and polymerisations [17]. Due to its favourable properties, *pulsed* ultrasound may also be used to generate emulsions and therefore increase the rate of reactions. Ultrasound may also be considered as a tool for green chemistry, by allowing the use of benign conditions and enhancing energy efficiency [18]. The use of ultrasound in high-pressure systems has been reported for several extraction processes in CO_2 [19–21].

A previous study by Timko et al. investigated the hydrolysis of benzoyl chloride in a CO_2/H_2O biphase under ultrasonication in a reactor of 87.2 cm^3 volume [22]. In the present study, we have designed a 1 dm^3 high-pressure ultrasound reactor and used this

* Corresponding author. Address: Chemical Engineering, University of Birmingham, Edgbaston, Birmingham, UK B15 2TT; Tel.: +44 (0) 7521998425.
E-mail address: g.a.leeke@bham.ac.uk (G.A. Leeke).

1350-4177
http://dx.doi.org/10.1016/j.ultsonch.2013.05.017

to emulsify a dense CO_2/H_2O solvent system. Scaling up the hydrolysis of benzoyl chloride, we show that the efficiency is not lost at this scale-up factor, highlighting the conservation of the positive physical effects of ultrasound. Emulsion formation and subsequent breakdown was observed by passing the emulsions through a 30 cm^3 view cell and monitoring the change in turbidity over time. The advantages of ultrasound were further demonstrated for the hydrolysis reaction in the presence of Tween 80, a bio-compatible surfactant, able to stabilise a uniform C/W emulsion with estimated surface areas greater than 480 $m^2\ kg^{-1}$. The combined effects of ultrasound and Tween 80 resulted in faster reaction rates than those reported for a pre-formed H_2O in CO_2 (W/C) microemulsion [23], with higher energy efficiency than without the use of surfactant. Overall, the results demonstrate the potential utility of this reactor methodology for industrial applications.

2. Materials and methods

2.1. Reagents

Benzaldehyde (>99%) [100-52-7], benzoyl chloride (>99%) [98-88-4], benzoic acid (>99%) [65-85-0], octane [111-65-9] and polysorbate [9005-65-6] (Tween 80), were purchased from Sigma–Aldrich UK, and used without further purification. Liquid carbon dioxide was obtained from BOC UK, CP grade, and had a given purity of 99.995%.

2.2. System configuration (Fig. 1)

A high-pressure, cylindrical 1 dm^3 stainless-steel vessel (Parr, USA I.D. = 9.5 cm, H = 16 cm) was designed to incorporate an ultrasound probe and manufactured for use in the present study. CO_2 was delivered to the vessel via a high-pressure pump (Thar Instruments), electronically connected to a PC. The amount of CO_2 entering the reactor was recorded via a mass flow meter positioned in-line before the pump. The vessel was insulated by an electric heating jacket, and the temperature was controlled by a temperature controller (Parr 4838) coupled to a J type thermocouple, positioned in an immersed thermowell. The pressure was recorded to within ±0.1 bar using a transducer (Druck PTX 1400; Druck Ltd, Leicester, UK) with dedicated display. Ultrasound was introduced from a 20 kHz VCX-1500W processor (Sonics & Materials, CT, USA), coupled with a titanium alloy horn of tip diameter 2 cm. Tip amplitude (20–100%) was manually selected and related to the energy transferred to the fluid, while the pulse rate could define the ratio of ultrasound ON/ultrasound OFF based on a sonication cycle (e.g. 25%, 1 s ON/3 s OFF). A calibration between delivered and dissipated power was undertaken using the calorimetric method [24]. Power density values reported here (W cm^{-3}) were obtained by dividing the total energy per pulse time (J s^{-1}) by the vessel volume. When comparing vessels of different sizes, power intensity (W cm^{-2}) may also be encountered. Here power intensity values were calculated by dividing the power by the irradiating surface area of the tip. As a consequence of high amplitude settings resulting in a rapid ~3 °C rise in the temperature of the vessel, water cooling was employed to keep the vessel temperature constant during experiments. A dual piston HPLC pump (Jasco PU-2087) with a maximum flow rate of 20 $cm^3\ min^{-1}$ was used to recirculate the vessel contents. Connections to the vessel were made by 1/4″ and 1/8″ stainless steel Swagelok tubing, while connections to the pump were made in 1/16″ tubing.

2.3. General method for sonication of the CO_2/H_2O biphase

The vessel was initially heated until the desired temperature (30 °C) was reached. Water was then added to give a volume between 400 and 650 mL. CO_2 was supplied to the sealed vessel at a flow rate of ~40 g min^{-1}, until the desired pressure was reached. Following 30 min of equilibration/recirculation, sonication was initiated and continued for a known time.

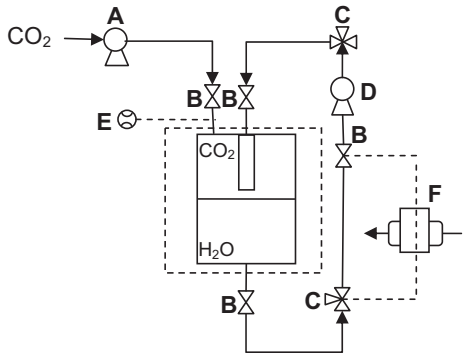

Fig. 1. Schematic showing the experimental setup utilised for sonication of CO_2/H_2O in the 1 dm^3 reactor A: CO_2 pump; B: high-pressure valve; C: 3-way sampling valve; D: circulation pump; E: 6-port valve for injecting compounds into the CO_2 stream; F: bypass of the H_2O recirculating line for visualisation through the 30 cm^3 view cell.

2.4. Observation of emulsion stability

A 30 cm^3 high-pressure stainless-steel view cell I.D. = 2.5 cm, H = 5.7 cm (Parr Instruments, Moline, IL, USA) fitted with two in-line sapphire windows (D = 1.5 cm), was used to visualise the dispersion generated in the ultrasound reactor (Fig. 1F), at 30 °C/80 bar. Heating was provided by two electric heating plates connected to a dedicated controller, and monitored by an immersed J type thermocouple. Emulsion stability was assessed by measuring the increase in light intensity (Visilight I-Led) over time, following termination of a 10-min sonication/circulation period. Time-lapse recordings were carried out using a Photron high-speed camera at 10-s time intervals, and the digital images transferred to a PC, using a dedicated interface. The images were analysed with ImageJ for the sum of the greyscale pixel values (integrated density) inside a defined area, and each time-point value divided by the maximum density recorded in the absence of turbidity. Experiments were also performed under conditions above the CO_2 critical point in order to minimise any effect associated with phase transition.

2.5. Compound injection, sampling and analysis

For greater precision, hydrophobic compounds were added to the CO_2 phase via a 6-port valve positioned in-line with the CO_2 feed, and connected by 1/16″ Swagelok tubing. A standard 1 mL bypass loop was used to inject a known amount of each compound. Following equilibration of the reactor contents at 30 °C/70 bar, either benzaldehyde or benzoyl chloride was injected into the flowing CO_2 feed, while final pressurisation to 80 bar was achieved. Aliquots (2 mL) were taken from the recirculating H_2O line at the specified time intervals and analysed immediately by gas chromatography (Shimadzu GC-2010, combined with autosampler and injector AOC-20, and equipped with a DB-5 column and an FID). Four or five aliquots were taken over the course of each experiment at different time points. For the same set of conditions, experiments were repeated three times, generating aggregated data of non-overlapping time points. The final concentration was obtained from a standard calibration line. The H_2O recirculating line originated from a 14-cm 1/4″ stainless steel dip tube immersed in the reactor. The sampling point was therefore positioned 8 cm below the probe tip. Aliquots from the CO_2 phase on the other hand were

taken from a line originating from a port at the top of the reactor, and were collected by slowly bubbling into cold acetone. In order to verify that all of the compounds tested were dissolved in the CO_2 phase prior to initiating sonication, visual experiments were conducted by injecting 100 μL of compound into the view cell charged with just CO_2. At the pressure and temperature described in this paper, only a single phase was observed.

2.6. Benzaldehyde mass transport

Mass transport experiments were conducted in order to assess the dispersive capacity of ultrasound for this vessel geometry (1 dm^3) using a hydrophobic compound, and to potentially compare mass transport rates with other systems reported in the literature. Benzaldehyde was chosen for the mass transport experiments as its solubility in CO_2 has been studied previously [25,26]. Moreover, it contains an important functional group for organic chemistry, namely the carbonyl group. The mass transport of benzaldehyde from CO_2 to H_2O was assessed by the two-film theory, previously described for similar systems by Timko [27], and Tai et al. [28][1].

Due to its influence on the mass transport, the partition coefficient was determined by measuring the concentrations of benzaldehyde partitioned in both phases, following 4 h of equilibration, and the resulting value was found to match to within 5% that reported in the literature (K_{CW} = 12) [29]. For comparison with values reported in the literature, the effective mass transport coefficient $K_{mtC}a*$ (s^{-1}) was calculated, where '$a*$' is the surface area per unit volume (cm^{-1}).

2.7. Kinetics of benzoyl chloride hydrolysis

The hydrolysis of benzoyl chloride represents a useful reaction for modelling kinetics in which a hydrophobic species (the acid chloride) must cross the interface, meet the hydrophilic species (H_2O), and react (Scheme 1). In the present system, the reverse case is also true, whereby H_2O travels to the CO_2 side and reacts with the acid chloride.

Initial rates of benzoyl chloride hydrolysis were analysed under amplitude settings of 20–70%, and were found to follow first-order kinetics, as previously reported [23,30].[1] The reaction was also studied in the presence of the surfactant polysorbate, Tween 80. This surfactant was chosen due to an existing in-depth knowledge of its C/W emulsion properties from the literature [31]. To this end, the same procedure was followed as that described above other than 0.5 or 1.0 wt.% of surfactant (with respect to water) was dissolved in the water prior to charging the vessel. Samples were taken at various time points, and the reaction was quenched by trapping the carboxylic acid hydrolysis product in acetone on ice (1:6 dilution by volume) before analysing by GC. As sonication in the presence of Tween resulted in a greater fraction of CO_2 being dispersed in H_2O compared to when sonication was carried out without Tween, a few considerations had to be made. To investigate whether or not the benzoic acid hydrolysis product had formed *in situ* as a result of ultrasound mixing, or by mixing during sample depressurisation, the same experimental protocol was carried out with an additional visual aid using the view cell. Following 1 min of sonication, ultrasound was stopped and the contents were recirculated until the emulsion reverted to the biphase. After 1 h, when only a clear solution was observed to pass through the view cell, samples were collected in the usual manner. The sample concentration closely paralleled that obtained from 1 min ongoing sonication, indicating that the benzoic acid had not formed as a consequence of the benzoyl chloride-containing emulsion rapidly breaking down upon depressurisation into the sample vial. The yields were plotted as a function of time at different ultrasound power settings.

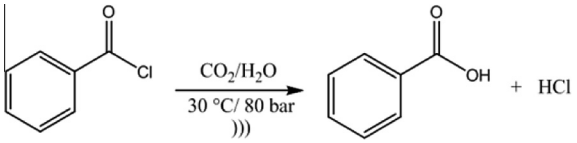

Scheme 1.

3. Results and discussion

3.1. Emulsion appearance and stability

Emulsions originating in the H_2O-continuous phase were assessed first. Approximately 10 min after commencing sonication, turbidity was observed to increase inside the view cell (Fig. 2a and b). Following the ceasing of sonication, this turbidity remained for approximately 30 min, gradually reverting to the biphase with a characteristic demulsification front (Fig. 2c). Droplets could be observed to collect on the upper part of the inside wall of the window, which increased in size and number over time, indicating that the emulsion was breaking down by CO_2 droplet coalescence.

Turbid emulsions generated by ultrasound were reported as being indicative of droplets with Sauter mean diameters of 9 μm for H_2O droplets in CO_2-continuous (W/C), and 15 μm for CO_2 droplets in H_2O-continuous (C/W) emulsions [22]. In our system, turbidity was observed regardless of whether the H_2O- or CO_2-continuous phase was recirculated through the view cell during sonication (Fig. 3). This allowed measurement of emulsion stability by assessing the decrease in turbidity in the view cell. The data points for the fastest increase observed in light intensity were plotted and found to fit a second-order polynomial function ($r^2 > 0.99$, Fig. 4). This was found to closely match the observed time course for emulsion breakdown visualised by eye. Volume fractions of CO_2 in H_2O were evaluated by the tracer technique,[1] and were found to be between 1% and 6%, depending on the standoff distance of the biphase line from the probe (Fig. 5). Optimal dispersion of CO_2 in H_2O was achieved when the biphase line was positioned between 1 cm and 2 cm below the probe surface. This observation was consistent with previous studies in liquids at ambient conditions that showed cavitation bubble velocity and bubble flow rate decrease dramatically in intensity at distances of more than 4 cm below the probe [32]. Emulsification may also result in H_2O droplets dispersing in the CO_2 phase. As a consequence, water collected from the CO_2-continuous phase revealed the H_2O volume fraction to be 6.5% (± 1) following sonication.

3.2. Mass transport

Following injection of 1 mL benzaldehyde, sample analysis revealed that its concentration measured in the upper part of the

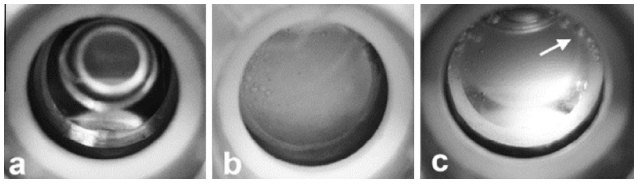

Fig. 2. Turbidity of the recirculating H_2O-continuous phase as observed through the view cell, following sonication in the 1 dm^3 high-pressure reactor. (a) Circulation, no sonication; (b) 10 min following the start of sonication (c) approximately 10 min after stopping sonication, CO_2 droplets collect on the upper inside wall (arrow). (Conditions: 30 °C/80 bar, 70% amplitude, 25% pulse rate).

[1] See supplementary data.

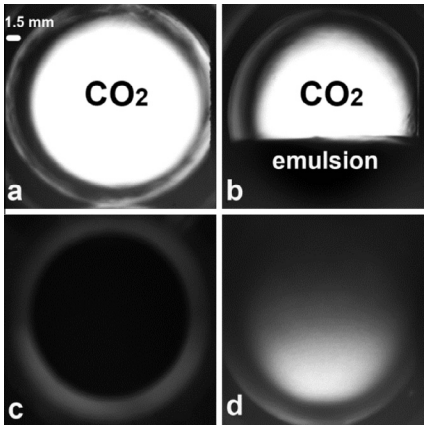

Fig. 3. Darkening of the recirculated CO_2-continuous phase through the view cell, following sonication in the 1 dm^3 high-pressure vessel: (a) for image analysis experiments, a light source was located at the rear window to illuminate the contents of the cell; (b) approximately 3 min after the start of sonication, a turbid phase was seen in the cell; (c) after 10 min of sonication/circulation, complete opacity was observed; (d) 5 min after stopping sonication, light transmittance was partially restored due to reversal to the biphase. Conditions: 30 °C/80 bar, 70% amplitude, 25% pulse rate.

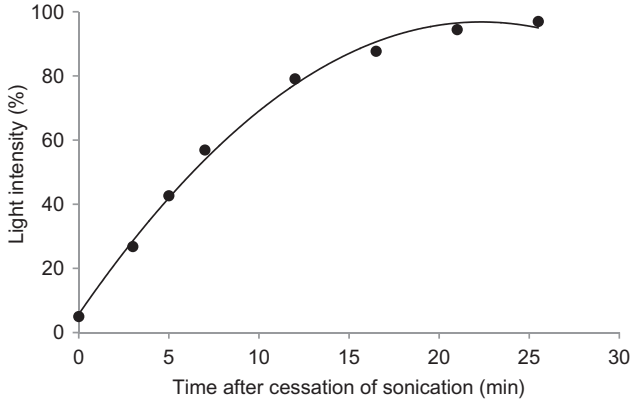

Fig. 4. Increase in light intensity through the view cell following termination of sonication, and reversal from emulsified to biphasic conditions. Conditions: 30 °C/80 bar, 70% amplitude, 25% pulse rate.

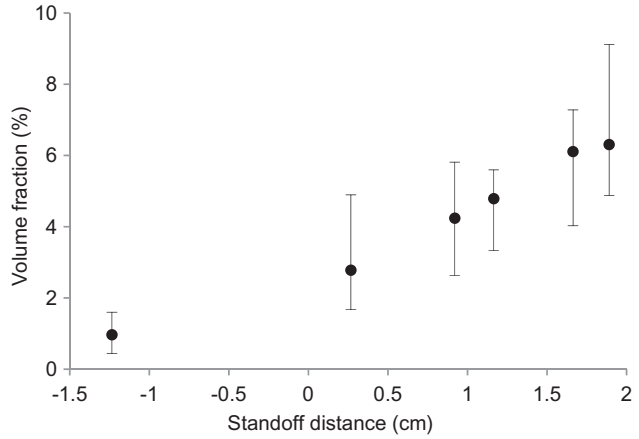

Fig. 5. Volume fractions of CO_2 dispersed in H_2O following sonication. The standoff distance signifies the position of the biphase line with respect to the probe. The negative values denote conditions in which the biphase line was above the probe surface (i.e. probe immersed in H_2O). The position of the biphase line was adjusted by changing the initial H_2O volume in the reactor, which was (from left to right): 800, 700, 650, 630, 600 and 580 mL H_2O. The number of experimental points for each standoff distance was between 3 and 7. No tracer was detected in the H_2O phase after 3 h of only recirculation. Conditions: 30°/80 bar, 70% amplitude, 25% pulse rate.

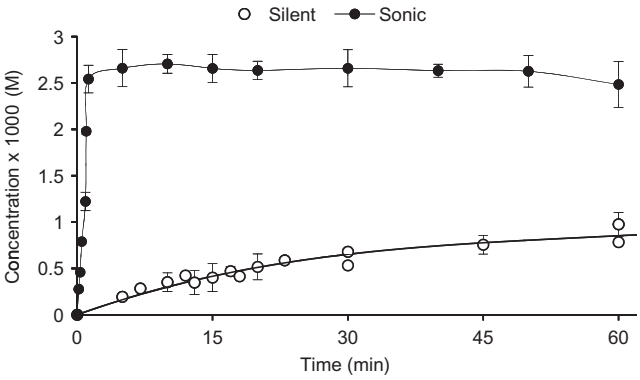

Fig. 6. Benzaldehyde concentration in samples from the H_2O-continuous phase for 'silent' and sonicated (70% amplitude, 25% pulse rate) environments. Conditions: 1 mL benzaldehyde (C_{C0} = 0.028 M), CO_2 = 25 wt% (220 g CO_2, 650 g H_2O), 30 °C/0 bar.

reactor during sonication was roughly ten times higher than that in the lower part. Together with volume fraction measurements from the previous section, the results indicated that two distinct environments existed simultaneously during sonication, one CO_2-continuous and one H_2O-continuous in the upper and lower parts of the reactor, respectively. The change of benzaldehyde concentration over time under only circulation ('silent') and under sonication conditions, is presented in Fig. 6. The equilibrium for benzaldehyde mass transport was reached within approximately 2 h under only circulation conditions, whereas it was reached within 1 min following the start of sonication. Analysis of the log plot yielded slopes of 2.7 and 0.023×10^{-2} s^{-1} for the sonicated and 'silent' case, respectively. Insertion of known parameters (V_W = 650 cm^3, V_C = 350 cm^3 and K_{CW} = 12), yielded respective $K_{mtC}a^*$ values of 1.9×10^{-3} s^{-1} and $\approx 0.016 \times 10^{-3}$ s^{-1}, and calculation of their ratio afforded a sonic enhancement factor of ~120. The value for the sonicated case was within the range for the transfer of most species in liquid–liquid mixtures. Tai et al. studied the impeller-induced mass transport of zinc(II) ions in a 1.3 dm^3 batch with a CO_2/H_2O biphase, reporting values of $0.2–2.6 \times 10^{-3}$ s^{-1} at impeller speeds of 400–1000 rpm at 40 °C/83 bar [28]. Mass transport is furthermore highly dependent on the type of contactor and agitation employed. For example, the effective mass transport coefficient ranged between 0.016 and 1.6×10^{-3} s^{-1} for a stirred tank, or as high as 30.6 s^{-1} in a microchannel [33]. In a different study, the effective gas–liquid mass transfer coefficient increased from ~0.1 to 10×10^{-3} s^{-1} when 500 rpm stirring was complemented with ultrasound in a 1 L vessel [34]. Separation of K_{mtC} into its H_2O and CO_2 components[2] (K_W and K_C respectively) revealed an estimated $K_W \approx 1.5 \pm 0.5 \times 10^{-4}$ cm s^{-1}. This value was found to be approximately half that reported for a 87.2 cm^3 vessel with a higher interfacial area to volume ratio, under gentle circulation (a/V_w = 3.7 higher [22]), and was within an order of magnitude for the transfer of most organic species in water. Hydrophobic compounds such as benzaldehyde are always expected to transfer through CO_2 faster than through H_2O, highlighting how pulsed ultrasound may be employed to enhance mass transport rates of such species through the interface, by almost two orders of magnitude.

[2] Once K_{mtc} was obtained from $K_{mtc}a^*$ (by inserting 'a' = 71 cm^2 and V_W = 650 cm^3), kw and kc were derived from the relation: $K_{mtc} = 1/(1/K_C + K_{CW}/K_W)$, and solved for $K_C/K_W \geq 9$.

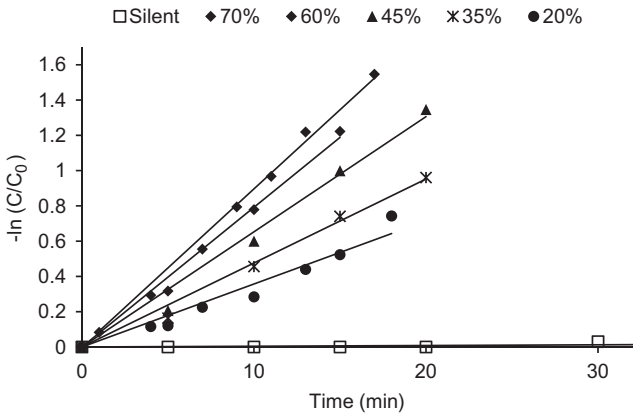

Fig. 7. Initial rate first-order plots for the hydrolysis of benzoyl chloride, under silent conditions or with sonication at different amplitude settings ($r^2 \geqslant 0.96$). Each value in the legend represents the amplitude setting. Conditions: C_{C0} = 0.025 M, W_{CO2} = 25% (220 g CO_2, 650 g H_2O), 30 °C/80 bar, pulse rate 25%.

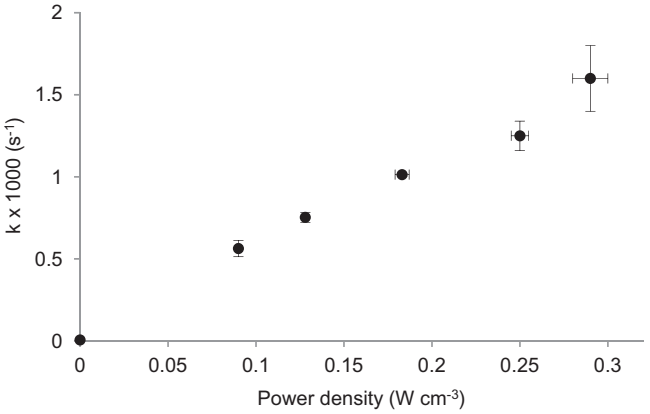

Fig. 8. Graph showing the relationship between the rate constant for benzoyl chloride hydrolysis, and ultrasound power density. Conditions: C_{C0} = 0.025 M, CO_2 = 25 wt.% (220 g CO_2, 650 g H_2O), 30 °C/80 bar, pulse rate 25%.

3.3. Scale-up feasibility by kinetics of benzoyl chloride hydrolysis

Hydrolysis represents an important reaction and is employed in the preparation of many pharmaceutical compounds [35]. A range of amplitude settings was used to study the hydrolysis of benzoyl chloride and for the calculation of the respective rate constants (Fig. 7).

Comparison with a smaller, 87.2 cm^3 reactor reported in the literature revealed that initial rates were similar for both systems at approximately equal power intensities (power intensity here was 95.5 W cm^{-2} with the 1500 W sonifier and a probe tip surface area of 3.14 cm^2, whereas for the smaller vessel the intensity was 104 W cm^{-2} with a 400 W sonifier and a probe tip surface area of 0.5 cm^2, Table 1, Entries 1, 2). In the study by Timko et al., no sonochemical effects by ultrasound were observed, inferring that faster hydrolysis rates were due to increased interfacial areas between CO_2 and H_2O. Further demonstration of the conservation of efficiency, was provided by observing an almost equivalent rise in the rate constant over the same range of power densities, for both vessel dimensions (rate constant increased roughly 3 times in the range 0.1–0.3 W cm^{-3}, Fig. 8) [30].

Scale-up of sonochemical processes is usually problematic due to their dependence on localised cavitation events (immediately below the irradiating probe), and wide variation in the energy dissipation in the bulk volume [24]. Scale-up operations may also be hindered by the fact that the progressive erosion and shortening of the probe may eventually lead to reduced efficiency and increased process costs [36]. However, ultrasound in high-pressure, and especially near-critical, fluids, displays distinct advantages compared to sonication of fluids under ambient conditions, including 'soft' cavitation (therefore limiting erosion of the probe tip), and increased biphasic interfacial disruption (better dispersive and micro-mixing capacity) due to the low surface tension, high vapour density and low liquid density of CO_2 [37,38]. Furthermore, in the vicinity of a heterogeneous surface, the acoustic wave leads to the generation of physical and mechanical phenomena such as acoustic streaming and microjetting, which may be beneficial regardless of any sonochemical effect taking place [39,40]. As a consequence, two immiscible liquids will generate an emulsion, which may not be solely localised beneath the irradiating surface once formed, but as in the present case, will occupy larger fractions of the vessel volume. Factors governing ultrasound efficiency for heterogeneous systems include distance of the biphase line from the probe (here with 650 cm^3 H_2O 75 wt.%, this was 1 cm below the ultrasound probe), probe surface area, and vessel geometry. An aluminium foil test [41] revealed that significant erosion took place at 1 cm below the probe, indicating the presence of cavitation events with a circular pattern and diameter (~1.2 cm) approximately equal to that of the probe (Fig. 9).

Ultrasound-induced cavitation in liquid CO_2 has proven to be beneficial in a number of applications, including the preparation of polymers, drug nanoparticles, and ceramic materials [42–44]. In this system, hydrolysis occurred in two distinct environments, a H_2O-continuous phase existing below the probe, where benzoyl chloride-containing CO_2 droplets were constantly being formed and reacted with surrounding H_2O, and a CO_2-continuous phase in which H_2O was constantly fluxing to react with benzoyl chloride (Scheme 2).

Table 1
Comparison of benzoyl chloride hydrolysis rates between various emulsion systems.

Entry	Conditions	k_{hyd} ($\times 10^3$ s^{-1})
1	C/W–W/C Ultrasound[a] Silent (This work)	1.6 ± 0.3 0.007
2	C/W W/C Ultrasound[b]	1.8 ± 0.2
3	C/W Ultrasound + Tween 80 (This work)[c]	6–16
4	Pre-formed W/C microemulsion[d]	0.064
5	Pre-formed O/W microemulsion[e]	4.14

[a] US 0.3 W cm^{-3}/95 W cm^{-2}, 1 dm^3 US reactor, 30 °C/80 bar CO_2/H_2O.
[b] US 0.6 W cm^{-3}/105 W cm^{-2}, 87 cm^3 US reactor, 30 °C/80 bar CO_2/H_2O [22].
[c] Measured from the initial linear portion of the plot.
[d] CO_2/PFPE/H_2O microemulsion 35 °C/276 bar [23].
[e] Isooctane/AOT(dioctyl sodium sulfosuccinate)/H_2O microemulsion, 25 °C/ambient pressure [50].

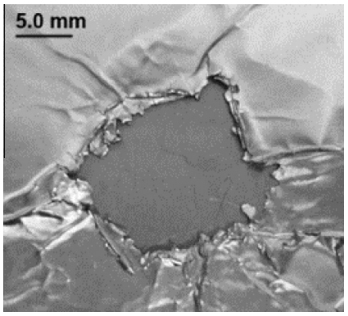

Fig. 9. Image of aluminium foil erosion following 1 min sonication in CO_2/H_2O. Four layers of foil were wrapped around a stainless steel plate positioned 1 cm below the probe. Conditions: CO_2/H_2O 50 v%, 30 °C/80 bar, 70% amplitude, 25% pulse rate.

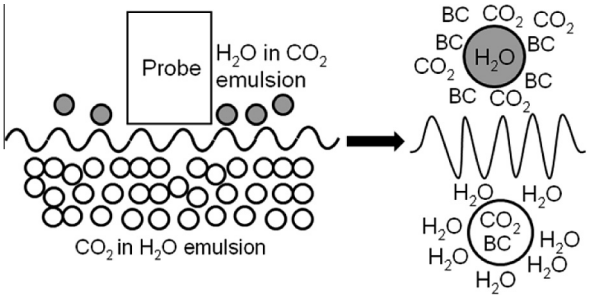

Scheme 2. Simplified diagram showing the simultaneous formation of CO_2 in H_2O and H_2O in CO_2 environments by ultrasound (left). The reaction may proceed in both environments, by the hydrophobic compound encountering a water droplet in the bulk CO_2 phase, or by the compound-carrying CO_2 droplet interacting with the bulk water phase (right, BC = benzoyl chloride).

As expected, the reaction proceeded faster under sonication compared to silent conditions, by effectively increasing the CO_2/H_2O interfacial area. Sonication with 70% amplitude afforded the maximum yield in 30 min (Fig. 11, dashed lines)[3]. In the absence of sonication, the hydrolysis of benzoyl chloride was extremely slow ($t_{1/2} \approx 27$ h). The sonic enhancement factor for hydrolysis rates relative to the silent case was therefore almost 230. When assessing reaction rates in binary solvent systems, hydrophobic interactions between the solvent and the reagent must also be taken into account; in this respect, ultrasound would alter the solvent structure and solvation [45], thus affecting the activation energy and entropy values for the reaction. Using different alcohol–water compositions, Salmar et al. showed that the solvent affected the rate constants depending on the alcohol/water fraction used, by hydrophobic stabilisation of either the transition complex or the ground state of the reagent [46].

The results from this part of the study highlight how the physical effects of ultrasound may be applied to include the efficient processing of high-pressure fluids on the litre scale, and may provide scope for identifying specific reaction pathways that may benefit from emulsification of H_2O-containing heterogeneous systems [47]. Furthermore, in this system, the reaction between CO_2 and H_2O formed a spontaneous acidic environment ($pH \leqslant 4$), potentially acting as an intrinsic catalyst that tends to neutral pH following CO_2 venting.

3.4. Emulsion formation using Tween 80

Sonication in the presence of 1.0 wt.% Tween 80 generated a uniform, white emulsion (Fig. 10). Analysis of samples taken from the upper, CO_2-continuous section of the reactor, following injection of 1 mL octane (a hydrophobic tracer that preferentially partitions in CO_2 [29]), showed a 2.5-fold increase in the concentration of octane during sonication that reverted to the biphase when sonication was ceased.

Additionally, the quantity of water present in these samples disappeared gradually following termination of ultrasound. Quantification of the water mass collected, in combination with octane concentrations, suggested that the emulsion consisted of 35 ± 2% CO_2 and 70 ± 5% H_2O by volume, which gradually reverted to a separated biphase approximately 1 h after ceasing sonication. Comparison of samples from the upper and lower sections of the reactor showed similar compositions, indicating uniformity throughout the reactor.

The hydrolysis reaction was next assessed in the presence of Tween.

[3] For all yields after 30 min, see supplementary data.

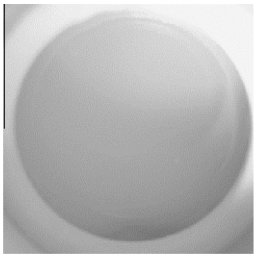

Fig. 10. Tween 80-stabilised (1.0 wt.%) emulsions generated by ultrasound. Conditions: CO_2 = 25 wt.% (220 g CO_2, 650 g H_2O), 30 °C/80 bar, after 10 min of ultrasound at 70% amplitude, 25% pulse rate.

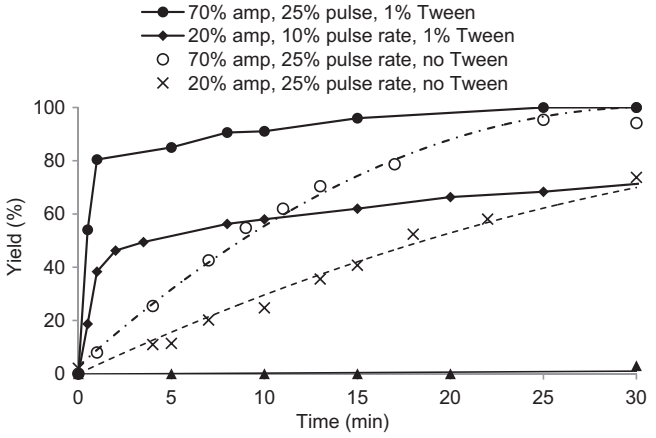

Fig. 11. Benzoyl chloride hydrolysis in Tween-stabilised (1.0 wt.%) C/W emulsions under different ultrasound conditions. Similar rates and yields were obtained with 0.5 wt.% Tween 80. Conditions: C_{C0} = 0.025 M, CO_2 = 25 wt.% (220 g CO_2, 650 g H_2O), 30 °C/80 bar.

Studies revealed that a combination of ultrasound and Tween was an effective environment for producing fast conversions of benzoyl chloride to benzoic acid (Fig. 11, solid lines).

Tween possesses an amphiphilic structure, and has been shown to stabilise C/W emulsions exclusively (even at 90 wt.% CO_2 for concentrated emulsions), with mean droplet diameters of 0.5–5.4 μm depending on the shear rates through a sand pack [31]. Confirmation of the C/W nature of the emulsion was obtained by injecting benzoyl chloride into the pre-formed emulsion, without further sonication, and analysing samples from both the upper and lower sections of the reactor. If the emulsion proved to be CO_2-continuous (W/C), substantial dissolution of either benzoyl chloride, benzoic acid, or both, would have occurred. The samples, however, contained neither species implying that following injection, benzoyl chloride encountered a H_2O-continuous phase, and due to its density (1.21 g cm^{-3}), resided at the bottom of the vessel without reacting. Tween-stabilised hydrolysis rates under ongoing sonication showed two distinct stages, the first achieving ~80% yield almost instantly, and a second showing slower conversion, reaching 100% yield after approximately 30 min. The rate of the Tween-stabilised hydrolysis could be controlled by manipulating the pulse rate. Pulsed ultrasound has distinct advantages over continuous ultrasound, such as an increase in the number of spatial reactive sites and residual pressure amplitude during the OFF stage of the cycle, and enhanced energy efficiency by decreased power draw [48,49]. Pulse rate may therefore be regarded as a valuable variable for process optimisation. Using 10% pulse rate and 20% amplitude, 100% yield of benzoic acid was reached within ~120 min, significantly slower than when higher pulse rates were

employed. Observation through the view cell revealed that turbidity was of a lower intensity and lagged by several minutes in reaching a maximum, suggesting that the emulsion consisted of a lower surface area during low pulse rate. At steady-state, assuming the highest mean CO_2 droplet diameter of 5 μm (as reported under conditions of shearing), and 35% volume of the dispersed phase, the total emulsion interfacial area was estimated[4] at 420 m^2 or 480 m^2 kg^{-1}.

Under the same conditions without Tween, surface areas for ultrasound-generated C/W and W/C emulsions were reported as 20 and 100 m^2 kg^{-1}, respectively, making the Tween-stabilised emulsion surface area at least four times higher [22]. However, surface area may not independently account for the large increase observed in hydrolysis rates. Additional ultrasound-induced effects such as convective forces on existing droplets, may define mass transport and reaction rates, with droplet size playing an important factor in droplet dynamics. In support of this, benzoyl chloride hydrolysis in a pre-formed W/C emulsion was much slower (Table 1, Entry 4).

Another advantage of using a surfactant is improved energy efficiency, as demonstrated by experiments using different pulse rates. After 5 min of sonication at 20% amplitude, inclusion of surfactant yielded a fivefold higher concentration in benzoic acid with a 2.5-times lower energy requirement (2700 J with 10% pulse rate compared to 6750 J with 25% pulse rate for sonication with and without surfactant, respectively). A combination of low pulse rate and surfactant may therefore offer a useful processing strategy for minimising energy expenditure without compromising the yield.

4. Conclusions

This study highlights two important aspects regarding the utilisation of ultrasound in high-pressure systems. First, processes that rely on the physical effects of sonication and lead to dispersion of heterogeneous phases may be safely scaled-up (over 11-fold in the present study) without loss of efficiency, due to less dependence on cavitation and the sonolytic effect which may quickly dissipate from the irradiating surface in larger vessels. Second, the effect of ultrasound may be complemented by including low quantities of a bio-compatible surfactant (as low as 0.5 wt.%), resulting in complete emulsification of the biphasic mixture, which maintains a defined C/W nature and uniformity throughout the reactor. It is therefore easy to envisage how the nature of the environment may be best suited to different applications either: (i) ongoing reaction/separation (without Tween two distinct environments co-exist, allowing preferential partitioning in the CO_2 and H_2O phases in real time), or (ii) complete emulsification forming only one type of environment (with Tween, achieving greater uniformity and surface area).

Appendix A. Supplementary data

Supplementary data associated with this article can be found, in the online version, at http://dx.doi.org/10.1016/j.ultsonch.2013.05.017.

[4] Surface area values were calculated according to the formula: $a = 6\phi / d_{32}$, where 'a' is the surface area (m^2), ϕ is the volume fraction (%) of the dispersed phase (or here simply volume, m^3), and d_{32} is the Sauter mean diameter of the droplet (m). The specific surface area (m^2 kg^{-1}) was obtained with respect to the total emulsion mass (0.87 kg).

References

[1] B. Cornils, W.A. Herrmann, R.W. Eckl, Industrial aspects of aqueous catalysis, J. Mol. Catal. A-Chem. 116 (1997) 27–33.
[2] J. Yoshida, K. Itami, Tag strategy for separation and recovery, Chem. Rev. 102 (2002) 3693–3716.
[3] J.-K. Lee, M.J. Fuchter, R.M. Williamson, G.A. Leeke, E.J. Bush, I.F. McConvey, S. Saubern, J.H. Ryan, A.B. Holmes, Diaryl ether synthesis in supercritical carbon dioxide in batch and continuous flow mode, Chem. Commun. 38 (2008) 4780–4782.
[4] R.A. Bourne, J.G. Stevens, J. Ke, M. Poliakoff, Maximising opportunities in supercritical chemistry: the continuous conversion of levulinic acid to γ-valerolactone in CO_2, Chem. Commun. (2007) 4632–4634.
[5] J.D. Holmes, K.J. Ziegler, M. Audriani, C.T. Lee, P.A. Bhargava, D.C. Steytler, K.P. Johnston, Buffering the aqueous phase pH in water-in-CO_2 microemulsions, J. Phys. Chem. B 103 (1999) 5703–5711.
[6] C. Roosen, M. Ansorge-Schumacher, T. Mang, W. Leitner, L. Greiner, Gaining pH-control in water/carbon dioxide biphasic systems, Green Chem. 9 (2007) 455–458.
[7] E.J. Beckman, Supercritical and near-critical CO_2 in green chemical synthesis and processing, J. Supercrit. Fluid 28 (2004) 121–191.
[8] K. Harrison, J. Goveas, K.P. Johnston, E.A. Orear, Water-in-carbon dioxide microemulsions with a fluorocarbon-hydrocarbon hybrid surfactant, Langmuir 10 (1994) 3536–3541.
[9] S.R.P. da Rocha, P.A. Psathas, E. Klein, K.P. Johnston, Concentrated CO_2-in-water emulsions with nonionic polymeric surfactants, J. Colloid Interf. Sci. 239 (2001) 241–253.
[10] D.J. McClements, Nanoemulsions versus microemulsions: terminology, differences, and similarities, Soft Matter 8 (2012) 1719–1729.
[11] G.B. Jacobson, C.T. Lee, K.P. Johnston, W. Tumas, Enhanced catalyst reactivity and separations using water/carbon dioxide emulsions, J. Am. Chem. Soc. 121 (1999) 11902–11903.
[12] H. Ohde, C.M. Wai, H. Kim, J. Kim, M. Ohde, Hydrogenation of olefins in supercritical CO_2 catalyzed by palladium nanoparticles in a water-in-CO_2 microemulsion, J. Am. Chem. Soc. 124 (2002) 4540–4541.
[13] R. Liu, C. Wu, Q. Wang, J. Ming, Y. Hao, Y. Yu, F. Zhao, Selective hydrogenation of citral catalyzed with palladium nanoparticles in CO_2-in-water emulsion, Green Chem. 11 (2009) 979–985.
[14] K. Burgemeister, G. Franciò, V.H. Gego, L. Greiner, H. Hugl, W. Leitner, Inverted supercritical carbon dioxide/aqueous biphasic media for rhodium-catalyzed hydrogenation reactions, Chem. Eur. J. 13 (2007) 2798–2804.
[15] M. McCarthy, H. Stemmer, W. Leitner, Catalysis in inverted supercritical CO_2/aqueous biphasic media, Green Chem. 4 (2002) 501–504.
[16] H. Ohde, F. Hunt, C.M. Wai, Synthesis of silver and copper nanoparticles in a water-in-supercritical-carbon dioxide microemulsion, Chem. Mater. 13 (2001) 4130–4135.
[17] R. Butler, I. Hopkinson, A.I. Cooper, Synthesis of porous emulsion-templated polymers using high internal phase CO_2-in-water emulsions, J. Am. Chem. Soc. 125 (2003) 14473–14481.
[18] T.J. Mason, Sonochemistry and sonoprocessing: the link, the trends and (probably) the future, Ultrason. Sonochem. 10 (2003) 175–179.
[19] Y. Gao, B. Nagy, X. Liu, B. Simandi, Q. Wang, Supercritical CO_2 extraction of lutein esters from marigold (Tagetes erecta L.) enhanced by ultrasound, J. Supercrit. Fluid 49 (2009) 345–350.
[20] S. Balachandran, S.E. Kentish, R. Mawson, M. Ashokkumar, Ultrasonic enhancement of the supercritical extraction from ginger, Ultrason. Sonochem. 13 (2006) 471–479.
[21] E. Riera, Y. Golas, A. Blanco, J.A. Gallego, M. Blasco, A. Mulet, Mass transfer enhancement in supercritical fluids extraction by means of power ultrasound, Ultrason. Sonochem. 11 (2004) 241–244.
[22] M.T. Timko, K.A. Smith, R.L. Danheiser, J.I. Steinfeld, J.W. Tester, Reaction rates in ultrasonic emulsions of dense carbon dioxide and water, AIChE J. 52 (2006) 1127–1141.
[23] G.B. Jacobson, C.T. Lee, K.P. Johnston, Organic synthesis in water carbon dioxide microemulsions, J. Org. Chem. 64 (1999) 1201–1206.
[24] P.R. Gogate, V.S. Sutkar, A.B. Pandit, Sonochemical reactors: important design and scale up considerations with a special emphasis on heterogeneous systems, Chem. Eng. J. 166 (2011) 1066–1082.
[25] D. Walther, G. Maurer, High-pressure vapor-liquid-equilibria in binary-mixtures of carbon-dioxide and benzaldehyde, bromobenzene, chlorobenzene, 1,2-dichlorobenzene and 2-chloro-1-methylbenzene at temperatures between 313-K and 393-K and pressures up to 22-MPa, Ber. Bunsen Phys. Chem. 96 (1992) 981–988.
[26] K.D. Wagner, K. Brudi, N. Dahmen, H. Schmieder, Partition coefficients of aromatic organic substances in two-phase mixtures of water and carbon dioxide at pressures from 8 to 30 MPa and at temperatures of 313 to 333 K. Part II, J. Supercrit. Fluid 15 (1999) 109–116.
[27] M.T. Timko, Acoustic emulsions of liquid, near-critical carbon dioxide and water: application to synthetic chemistry through reaction engineering, Ph.D Dissertation, Massachusetts Institute of Technology, 2004.
[28] C.Y. Tai, G.S. You, S.L. Chen, Kinetics study on supercritical fluid extraction of zinc(II) ion from aqueous solutions, J. Supercrit. Fluid 18 (2000) 201–212.
[29] M.T. Timko, B.F. Nicholson, J.I. Steinfeld, K.A. Smith, J.W. Tester, Partition coefficients of organic solutes between supercritical carbon dioxide and water: experimental measurements and empirical correlations, J. Chem. Eng. Data 49 (2004) 768–778.

[30] M.T. Timko, J.M. Diffendal, J.W. Tester, K.A. Smith, W.A. Peters, R.L. Danheiser, J.I. Steinfeld, Ultrasonic emulsification of liquid, near-critical carbon dioxide-water biphasic mixtures for acceleration of a hydrolysis reaction, J. Phys. Chem. A 107 (2003) 5503–5507.
[31] E. Torino, E. Reverchon, K.P. Johnston, Carbon dioxide/water, water/carbon dioxide emulsions and double emulsions stabilized with a nonionic biocompatible surfactant, J. Colloid Interf. Sci. 348 (2010) 469–478.
[32] N.A. Tsochatzidis, P. Guiraud, A.M. Wilhelm, H. Delmas, Determination of velocity, size and concentration of ultrasonic cavitation bubbles by the phase-Doppler technique, Chem. Eng. Sci. 56 (2001) 1831–1840.
[33] Y. Su, G. Chen, Y. Zhao, Q. Yuan, Intensification of liquid–liquid two-phase mass transfer by gas agitation in a microchannel, AIChE J. 55 (2009) 1948–1958.
[34] F. Laugier, C. Andriantsiferana, A.M. Wilhelm, H. Delmas, Ultrasound in gas-liquid systems: effects on solubility and mass transfer, Ultrason. Sonochem. 15 (2008) 965–972.
[35] V.Y. Kukushkin, A.J.L. Pombeiro, Metal-mediated and metal-catalyzed hydrolysis of nitriles, Inorg. Chim. Acta 358 (2005) 1–21.
[36] T.J. Mason, Practical Sonochemistry: User's Guide to Applications in Chemistry and Chemical Engineering, first ed., Ellis Horwood, Chichester, U.K., 1991.
[37] M.M. van Iersel, R. Mettin, N.E. Benes, D. Schwarzer, J.T.F. Keurentjes, Sound-driven fluid dynamics in pressurized carbon dioxide, J. Chem. Phys. 133 (2010) 044304.
[38] D.L. Goldfarb, H.R. Corti, F. Marken, R.G. Compton, High-pressure sonoelectrochemistry in aqueous solution: soft cavitation under CO_2, J. Phys. Chem. A 102 (1998) 8888–8893.
[39] D.G. Shchukin, E. Skorb, V. Belova, H. Möhwald, Ultrasonic cavitation at solid surfaces, Adv. Mater. 23 (2011) 1922–1934.
[40] A. Kumar, P.R. Gogate, A.B. Pandit, Mapping the efficacy of new designs for large scale sonochemical reactors, Ultrason. Sonochem. 14 (2007) 538–544.
[41] V. Saez, A. Frias-Ferrer, J. Iniesta, J. Gonzalez-Garcia, A. Aldaz, E. Riera, Chacterization of a 20 kHz sonoreactor. Part I: analysis of mechanical effects by classical and numerical methods, Ultrason. Sonochem. 12 (2005) 59–65.
[42] M.W.A. Kuijpers, D. van Eck, M.F. Kemmere, J.T.F. Keurentjes, Cavitation-induced reactions in high-pressure carbon dioxide, Science 298 (2002) 1969–1971.
[43] G.P. Sanganwar, R.B. Gupta, Nano-mixing of dipyridamole drug and excipient nanoparticles by sonication in liquid CO_2, Powder Technol. 196 (2009) 36–49.
[44] K. Matsuyama, K. Mishima, T. Kato, K. Ohara, Formation of porous glass via core/shell-structured poly(methyl methacrylate)/powder glass prepared by ultrasonic irradiation in liquid CO_2, J. Supercrit. Fluid 57 (2011) 198–206.
[45] A. Tuulmets, S. Salmar, Effect of ultrasound on ester hydrolysis in aqueous ethanol, Ultrason. Sonochem. 8 (2001) 209–212.
[46] A. Tuulmets, H. Hagu, S. Salmar, G. Cravotto, J. Jarv, Ultrasonic evidence of hydrophobic interactions. Effect of ultrasound on benzoin condensation and some other reactions in aqueous ethanol, J. Phys. Chem. B 111 (2007) 3133–3138.
[47] G. Cravotto, P. Cintas, Harnessing mechanochemical effects with ultrasound-induced reactions, Chem. Sci. 3 (2012) 295–307.
[48] T. Tuziuti, K. Yasui, J. Lee, T. Kozuka, A. Towata, Y. Iida, Mechanism of enhancement of sonochemical-reaction efficiency by pulsed ultrasound, J. Phys. Chem. A 112 (2008) 4875–4878.
[49] L.A. Gonzalez, P. Kracke, W.H. Green, J.W. Tester, L.M. Shafer, M.T. Timko, Oxidative desulfurization of middle-distillate fuels using activated carbon and power ultrasound, Energy Fuel. 26 (2012) 5164–5176.
[50] L. Garcia-Rio, J.R. Leis, J.A. Moreira, Reactivity in water/oil microemulsions. Influence of sodium bis(2-ethylhexyl)sulfosuccinate/isooctane/water microemulsions on the solvolysis mechanism of substituted benzoyl chlorides, J. Am. Chem. Soc. 122 (2000) 10325–10334.